# Optical properties of strongly coupled $Yb^{2+}$ and $CN^-$ ions in alkali halide crystals: Electronic absorption and emission

C. P. An, Volkmar Dierolf,* and Fritz Luty
*Department of Physics, University of Utah, Salt Lake City, Utah 84112*
(Received 22 October 1999)

We have studied absorption and emission spectra of the $4f^{14} \leftrightarrow 4f^{13}5d$ electronic transitions of $Yb^{2+}:(CN^-)_n$ defect complexes in NaCl, KCl, RbCl, and KBr host crystals under concentration variation of both dopants $Yb^{2+}$ and $CN^-$. Due to strong coupling between $Yb^{2+}$ and $(CN^-)_n$, the $Yb^{2+}$ electronic transitions shift drastically towards lower energies (from near uv to near ir) as the $n$ value increases. Applying thermal quenching and excitation spectroscopy of the emission, the observed absorption spectra can be decomposed into contributions from the various defect complexes $Yb^{2+}:(CN^-)_n$ with $n=0,1$, and $n \geqslant 2$. Within the framework of ligand field theory we can estimate a splitting parameter $D_q$ as high as $\sim 3450\ cm^{-1}$ for the $Yb^{2+}:(CN^-)_6$ complexes in KCN, a value three times higher than for isolated $Yb^{2+}$ defects in KCl. These large $D_q$ values can be understood by a comparison with other metal ion complexes and by the special role of $CN^-$ within the spectrochemical series. For our system we try to interpret the latter by a charge redistribution from the n $CN^-$ molecules to the $5d$ orbital of their $Yb^{2+}$ defect partner.

## I. INTRODUCTION

Diatomic $CN^-$ molecules substituted into alkali-halide crystals have several unique properties (a) Their concentration $x$ can be continuously increased from isolated defects ($x \ll 1$) up to a perfect molecular sublattice ($x=1$) in several hosts. (b) Relaxation of their stretching mode (at $\sim 5\ \mu m$ or 0.25 eV) occurs mostly as a slow (ms) radiative process emitting vibrational luminescence (VL). (c) Neighboring electronic defects of $CN^-$ ions can under photo-excitation transfer electronic energy into the $CN^-$ stretching-mode and efficiently produce VL.

As most suitable electronic defect for process (c), the $F$ center was first introduced,[1] thoroughly investigated with various techniques,[2–5] and developed into the first successful demonstration of vibrational solid state laser.[6] In spite of simplicity and extensive studies of this $F$ center/$CN^-$ defect pair, full understanding of its internal $E$-$V$ energy transfer mechanism has not yet been achieved. This is due to the fact that origin of this energy transfer, caused by strongest mutual interaction and change of the individual properties of both partners, occurs only during or after relaxation of the excited $F$ center on a time scale so rapidly that it is extremely difficult to be followed experimentally.[5,7] More recently, several attempts to replace the $F$ center as ''energy donor'' for the $CN^-$ ion by other electronic defects have been started. Successful VL observation of $CN^-$ has been achieved by exciting the uv absorption of $Eu^{2+}$, $Tl^+$, and $Pb^{2+}$ defects in $CN^-$ doped KCl and KI crystals.[8,9] Similarly, $Yb^{2+}$ defects in KCl: $CN^-$ have been reported to show under $\sim 3$ eV excitation a broad VL emission around $4.8\ \mu m$.[10] In all these cases, however, the limitation of data (e.g., lack of kinetics study and/or spectral VL resolution) still prevented understanding of the underlying coupling and energy transfer mechanism.

In this work we have chosen the divalent rare earth $Yb^{2+}$ ion (accompanied by a cation vacancy for charge compensation) as the most interesting and promising alternative to the $F$ center for a comprehensive study in four hosts (NaCl, KCl, RbCl, and KBr). It is particularly challenging to study and understand coupling and $E$-$V$ energy-transfer for an electronic defect so different in its properties from that of $F$ centers. In contrast to the rather extended hydrogenlike wave functions with strong phonon-coupling of $F$ centers, the lowest optical transition of $Yb^{2+}(4f \rightarrow 5d)$ occurs between rather compact states of much lower phonon coupling. As its electronic luminescence EL (produced by photo excitation of its absorption manifold) has a long ($\sim$ ms) lifetime, study of the time dependence of energy transfer and EL versus VL competition appears particularly attractive. Much more than for $F$ center/$CN^-$ pairs, a strong mutual interaction changes drastically the properties of both individual $Yb^{2+}$ and $CN^-$ partners. We test this by variation of $CN^-$ concentration $x$ over the whole range (from $x=0$ up to 1, pure KCN). Motivated by this brief survey, we present this extended work in three consecutive parts,

(I) Electronic absorption (EA) and luminescence (EL) of $Yb^{2+}$ defects and their drastic change by coupling to one or more $CN^-$ partners, starting as a ''basis'' at $x=0$ and pursuing up to $x=1$.

(II) Vibrational absorption (VA) of $CN^-$ in various in configurations with $Yb^{2+}$ partners, and spectroscopy of its vibrational luminescence (VL), produced by E-V transfer from photoexcited $Yb^{2+}$.

(III) Study of time dependence of the energy transfer in terms of competition between EL of $Yb^{2+}$ and VL of $CN^-$ and its temperature dependence.

The properties and phenomena described in these three parts are often treated with theoretical models and viewpoints originating from different fields of solid state physics and chemistry. We still will try to unify them and introduce a phenomenological model which expresses the mutual coupling of the defects and their energy transfer in a common picture.

 

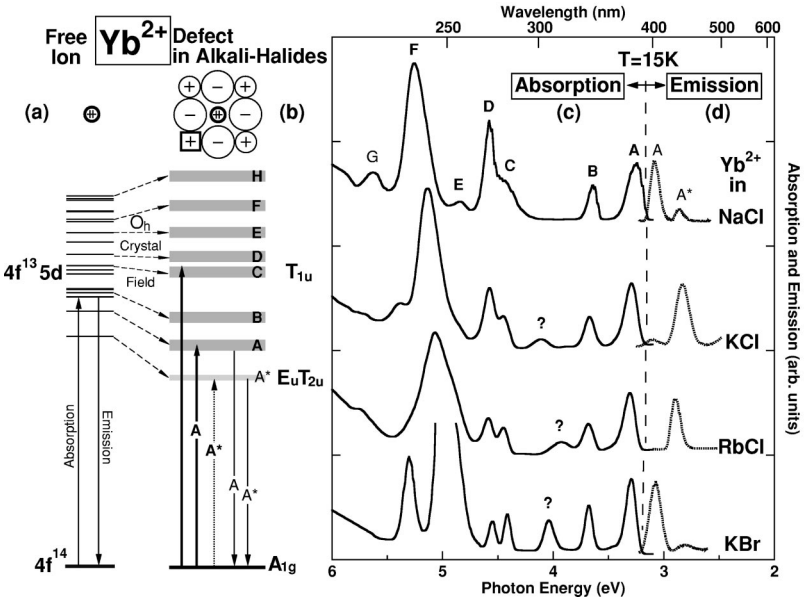


FIG. 1. $4f^{14} \rightarrow 4f^{13}5d$ electronic transitions of $Yb^{2+}$ ions: Schematic energy diagram of (a) free $Yb^{2+}$ ions and (b) isolated $Yb^{2+}$ in alkali halides. (c) Absorption and (d) emission (excited at 320 nm) spectra in NaCl, KCl, RbCl, and KBr hosts at $T=15$ K

In the first part we will start in the following by summarizing the essential properties of isolated $Yb^{2+}$ defects in alkali halides. On that basis we will present the experimental results for the $Yb^{2+}$-$CN^-$ complexes which will be discussed in the final discussion section.

## II. EXPERIMENTAL RESULTS

### A. Crystal growth and sample characterization

All $Yb^{2+}$ doped crystals studied in this work were grown in the Utah Crystal Growth Lab by the Kyropolous technique under hydrogen gas treatment, which converted the trivalent $Yb^{3+}$ supplied by the used $YbCl_3$ or $YbBr_3$ doping material into the divalent form. For codoping with $CN^-$ molecules, pure alkali-cyanide powder (of the same cation as the host material) was used. In many cases this material was added in one or two consecutive steps during crystal growth to the melt yielding, e.g., an $Yb^{2+}$ doped crystal which contains in part (A) no $CN^-$ and in part (B) and (C) increasing amounts of codoped $CN^-$. The simple ''observation with the eye'' of change from totally uncolored transparency to increasing yellow coloration among crystal parts A, B, and C was matched by observing the same change in color occurring already in the melt by $CN^-$ codoping. For the extreme case of $Yb^{2+}$ doped pure KCN as host both the melt and the resulting crystal appear nearly intransparent with a strong brown color. The mole concentration of defects in relevant crystal parts were determined for $[Yb^{2+}]$ by flame emission analysis, and for $[CN^-]$ by infrared absorption of its fundamental or second harmonic stretching mode. The ''distribution coefficient'' (ratio of concentration in crystal and melt) obtained from doping with $Yb^{2+}$ alone, varies strongly with the cation size of the host, yielding 0.2 for NaCl, 0.05 for KCl, and 0.01 for RbCl. In the latter three hosts we found considerable increases of these values (up to a factor 4) when codoping the melt with increasing amounts of $CN^-$.

### B. Isolated $Yb^{2+}$ defects in alkali-halide hosts

In Fig. 1 we illustrate and summarize the properties of $Yb^{2+}$ electronic states and optical transitions which are most essential for this work. It is well established for free $Yb^{2+}$ ions,[11] that the lowest allowed optical transitions from its closed-shell $4f^{14}$ ground state take place (with different relative strengths) into the numerous sublevels of the $4f^{13}5d$ excited state [Fig. 1(a)]. When substituted as a defect in an ionic crystal, the strong electro-static forces on these states from the ''point-ion'' crystal field of strength $D_q$ and symmetry must be considered. In alkali-halide hosts, the substitutional $O_h$ site symmetry of $Yb^{2+}$ becomes in principle lowered to $C_{2v}$ due to the charge-compensating cation-vacancy attached in the $\langle 110 \rangle$ direction. However, the perturbation from this vacancy on the optical transition is negligibly small, because the excited state electronic orbitals interact predominantly with the oppositely charged six nearest neighbor anions. Consequently, theoretical treatments with an $O_h$ crystal field are quite appropriate,[12,13] and yield very similar results as for $Yb^{2+}$ without vacancy in divalent ionic crystals,[14] such as $SrCl_2$.

Figure 1(b) illustrates schematically the result of calculations with an $O_h$ crystal field of appropriately chosen strength: According to the Hund's rule the $4f^{14}$ ground state is of $A_{1g}$ symmetry and therefore only transitions to the 18 $(5d)$ states with $T_{1u}$ symmetry are allowed and give contributions to the absorption spectrum. We mark (following Ref. 13) these phonon-broadened bands by bold alphabetic notation (**A**,**B**, . . . , for absorption and $A$ for emission). The lowest energy $^3P_2$ term forms two $E_u$ and $T_{2u}$ states of very small separation and hence absorption (**A***) and emission ($A^*$) transitions between $A_{1g}$ and these states should in principle be forbidden.

How do these theoretical predictions compare with experimental results? Figure 1(c) shows the uv-visible absorption spectra of $Yb^{2+}$ defects, measured (with a Cary 17D spectrometer) for low $Yb^{2+}$ concentrations in four different hosts at 15 K. Our measured $Yb^{2+}$ spectra in Fig. 1(c) agree

quite closely with the absorption results reported and partially analyzed in earlier papers.[12,13,15] Characteristic to these systems is a multiband structure (labeled **A**,**B**,**C**, . . . ) which changes only by small shifts or broadening effects under host material variation NaCl, KCl, RbCl, and KBr. Most of these observed bands can be explained and fitted quite well in position and strength by $4f^{14} \rightarrow 4f^{13}5d$ transitions of $Yb^{2+}$ in an $O_h$ crystal field, whose strength parameter $D_q$ varies only slightly (around $D_q \approx 1200\ cm^{-1}$) in these four hosts.[12] Exceptions from this statement are the observed **G** band and the question-marked band between **B** and **C**, which cannot be fitted by this model. Their different origin is confirmed by our observation in Fig. 1(c) that their position and strength change strongly under host variation. Presence and behavior of these bands is most likely due to covalency, i.e., a partial transfer of charge from the neighboring anions to the $Yb^{2+}$ defect. We will treat this effect in more detail in Sec. III when discussing the drastic changes of optical transitions by neighboring $CN^-$ ions.

In part (d) of Fig. 1 we summarize the $Yb^{2+}$ emission spectra in the four hosts at 15 K, produced by excitation at 310 nm with a pulsed excimer-dye laser, and detected with a Si detector behind an ARIES FF250 spectrograph. Only for the NaCl host, this emission spectrum has been observed[13] and interpreted[16] in previous works. It consists at low T of two emission bands *A* and *A** (called I and II bands in Ref. 16). The strong *A* emission band is the mirror image of the **A**-absorption band around a common zero-phonon line. Separated from the *A* emission by $\sim 2000\ cm^{-1}$ or 250 meV appears a weak emission band (*A**). The qualitative interpretation in NaCl can be easily understood from the level scheme in Fig. 1(b): After excitation into any of the higher absorption bands (**B**,**C**, . . . ) the system relaxes nonradiatively into the lowest $T_{1u}$ state. Originating from this state the strong *A* emission with a fast radiative rate ($\sim \mu s$) is observed. At low temperature only a small fraction of ions relaxes nonradiatively into the $E_u$ and $T_{2u}$ states resulting in a weak *A** emission with a slow rate $\tau_{A*} \approx 7 \times 10^2\ sec^{-1}$.

In addition to the full agreement with these earlier results in NaCl, Fig. 1(d) shows for the KBr host basically the same (*A* emission dominated) behavior as in NaCl. In contrast to this, the $A \rightarrow A^*$ relaxation is obviously much more efficient in KCl and RbCl, eliminating nearly totally the *A* emission on the expense of a strong *A** emission. Observation of this symmetry-forbidden *A** emission ($E_u$ and $T_{2u} \rightarrow A_{1g}$), encouraged our attempt to detect also the opposite **A*** absorption process (never reported in any previous paper). We tried this for $Yb^{2+}$ in NaCl, KCl, and KBr hosts, whose strong *A* band absorptions at 15 K are shown in Fig. 2(a). When creating a large (100–2500) ''amplification factor'' by use of thicker crystals with higher $[Yb^{2+}]$ concentrations ($\sim 10^{-3}$), we observe indeed in all three cases a weak **A*** absorption shown in Fig. 2(b). The obtained energy separation of the **A** and **A*** absorptions ($\sim 280$ meV) is very similar to that of the *A* and *A** emission shown in Fig. 1(d). For NaCl, the **A**/**A*** integrated absorption ratio of $\sim 400$ in Fig. 2 agrees closely with the $\sim 500$ ratio of *A*/*A** emission rates measured at 20 K in Ref. 16. The higher absorption ratios ($\sim$ 3000 and 1000) in KCl and KBr, respectively, observed in Fig. 2, predict similarly higher ratios of *A*/*A** emission rates in these hosts. Different from the low-resolution survey

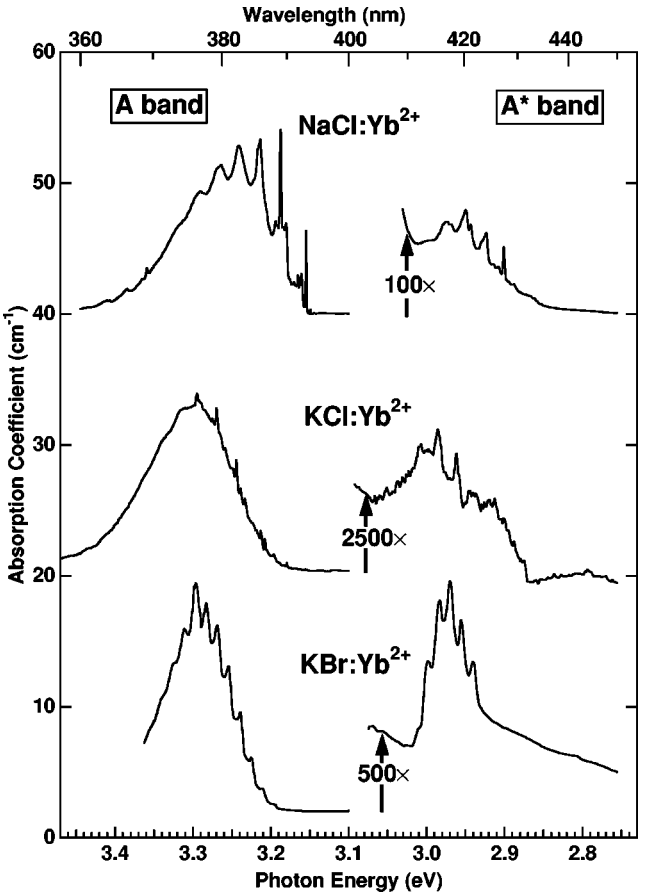


FIG. 2. Absorption spectra of the **A** and **A*** (expanded scale) bands for isolated $Yb^{2+}$ defects in NaCl, KCl, and KBr hosts at $T = 15$ K.

measurements in Fig. 1(c), the high spectral resolution used in Fig. 2 reveals resolved vibronic substructure of the absorptions due to the rather weak electron-phonon coupling. This has been extensively measured and analyzed for the **A** band in terms of coupling to pseudo-localized modes.[15] For the **A*** absorption we find a similar vibronic structure reflecting a coupling to modes with frequencies equal within experimental error to the ones observed for the **A** absorption ($\sim 210\ cm^{-1}$ in NaCl and KCl, and quite smaller $\sim 115\ cm^{-1}$ in KBr).

### C. $Yb^{2+}$:$(CN^-)_n$ defect complexes in alkali-halide hosts

#### *1. Absorption and emission spectra*

In contrast to the very small variation of $Yb^{2+}$ absorption and emission spectra in four different hosts, Figs. 3 and 4 show their drastic changes under substitution of host anions by $CN^-$ ions. In Fig. 3 we illustrate the absorption and emission spectra of $Yb^{2+}$ in $[KCl]_{1-x}[KCN]_x$ and $[KBr]_{1-x}[KCN]_x$ hosts under variation of $x$ in four steps from $x = 0$ (pure KCl or KBr) to $x = 1$ (pure KCN). All these results were obtained at 15 K (except the case of $x = 1$, measured at 190 K due to the strong light scattering by the elastically ordered domains of KCN below 168 K). For easy comparison in Fig. 3 each measured spectrum is normalized to the $[Yb^{2+}]$ concentration of about $10^{-4}$. For $x = 10^{-3}$ new, weak, and quite broad $Yb^{2+}$ related absorption bands

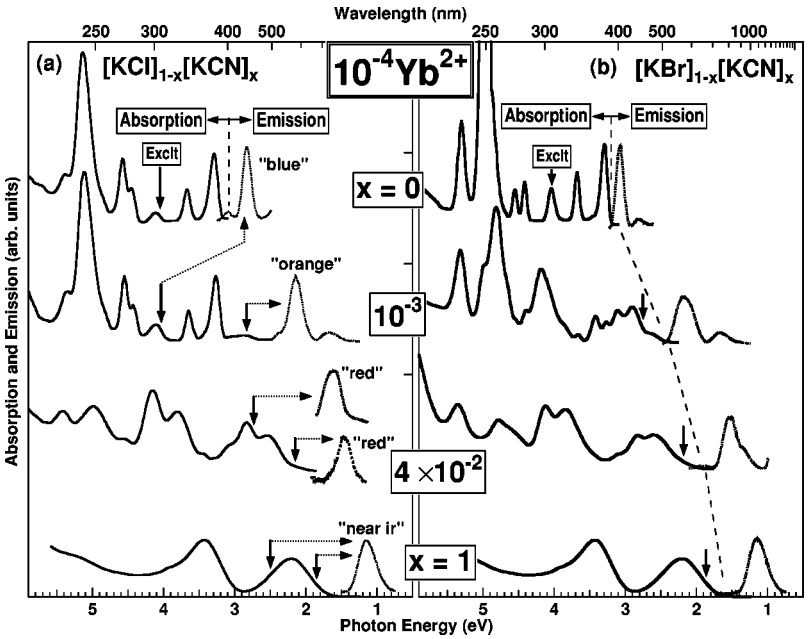


FIG. 3. Absorption and emission spectra for $4f^{14}\rightarrow 4f^{13}5d$ electronic transitions of $Yb^{2+}:(CN^-)_n$ defect complexes in KCl (a) and KBr (b) hosts at $T=15$ K under $[CN^-]$ concentration variation. Absorption intensities are normalized to $[Yb^{2+}]=10^{-4}$.

appear at the low energy side of the **A** band from isolated $Yb^{2+}$. Optical excitation of this sample at $\sim$ 310 nm produces the ''blue'' $A^*$ emission at $\sim$ 450 nm typical for isolated defects (shown in Fig. 1). On the other hand, excitation at $\sim$430 nm within the new absorption bands yields a new very bright emission ''orange'' with a maximum at $\sim$580 nm. This behavior reflects the fact that for small $x$ most of $Yb^{2+}$ ions still exist in this host crystal as isolated defects; only a small amount of $Yb^{2+}$ ions form defect pairs with $CN^-$ ions as neighbors. Assuming that the complexes involve only a single $CN^-$ ion and the total oscillator strengths of the absorption remains unchanged, we obtain an estimated concentration ratio of $[Yb^{2+}:CN^-]/[\text{isolated } Yb^{2+}]$ slightly higher than expected from statistics. As $x$ increases to 0.04, the new absorption bands become stronger and extend to even lower energies. Optical excitation of this sample at $\sim$460 nm and $\sim$590 nm produces a ''red'' emission at $\sim$780 nm. For the pure KCN host with the maximum value of $x$ the most drastic spectral changes are observed yielding for the lowest energy absorption band a peak position at 2.2 eV and an emission at 1.1 eV. In this case all $Yb^{2+}$ defects are surrounded by $n=6$ $CN^-$ neighbors, i.e., we only have $Yb^{2+}:(CN^-)_6$ complexes. Overall, we observe the clear trend that the red shift of absorption and emission increases with concentration of $CN^-$ ions and hence with the number $n$ of $CN^-$ neighbors for the $Yb^{2+}$ ions.

The absorption and emission spectra in NaCl and RbCl shown in Fig. 4 are very similar to those in KCl and KBr, again revealing an almost identical shift of the transition energies under increasing $[CN^-]$ concentration. As the only major difference we note that the amount of isolated $Yb^{2+}$ ions is considerably higher in NaCl compared to the other host materials. The reason for this are two facts, mentioned already in Sec. II A. As $Yb^{2+}$ is of nearly equal ionic size as $Na^+$, isolated $Yb^{2+}$ ions can enter from the melt into the

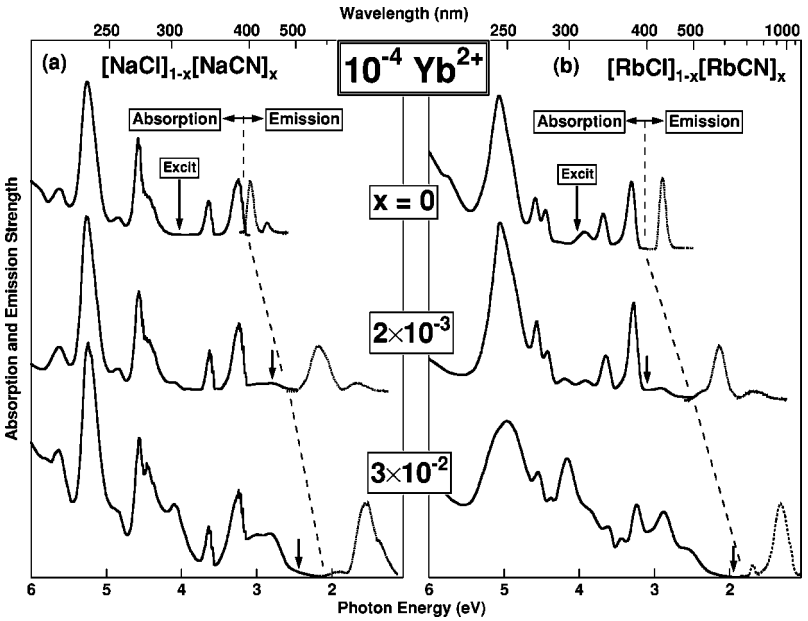


FIG. 4. Absorption and emission spectra for $4f^{14}\rightarrow 4f^{13}5d$ electronic transitions of $Yb^{2+}:(CN^-)_n$ defect complexes in NaCl (a) and RbCl (b) hosts at $T=15$ K under $[CN^-]$ concentration variation. Absorption intensities are normalized to $[Yb^{2+}]=10^{-4}$.

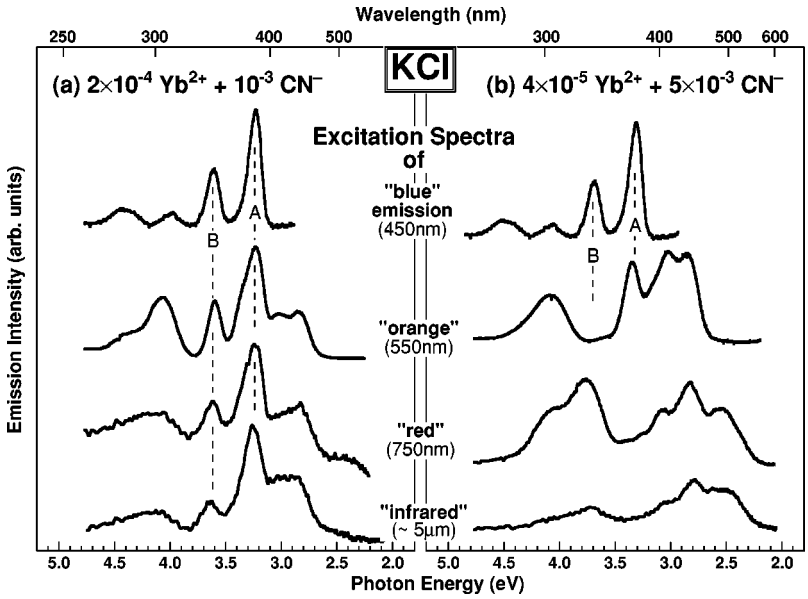


FIG. 5. Excitation spectra of blue, orange, red, and infrared emissions at $T=15$ K. (a) $KCl+2\times10^{-4}Yb^{2+}+10^{-3}CN^{-}$ (high $[Yb^{2+}]$ and low $[CN^{-}]$) and (b) $KCl+4\times10^{-5}Yb^{2+}+5\times10^{-3}CN^{-}$ (low $[Yb^{2+}]$ and high $[CN^{-}]$).

solid with high distribution coefficient for NaCl, but are much more rejected in $K^{+}$ and $Rb^{+}$ halides due to ''size misfit.'' On the other hand $Yb^{2+}$-$CN^{-}$ pairs which exist already in the melt, enter best into the solid when their pair-size fits well into that of two neighboring lattice ions. This leads, e.g., in RbCl hosts to a $\sim4$ times higher distribution coefficient for pairs compared to isolated $Yb^{2+}$ ions.

For a more systematic analysis of the spectral shifts, it is necessary to decompose the measured absorption and emission spectra into the individual spectra of $Yb^{2+}$: $(CN^{-})_n$ complexes with a certain $n$ value. This decomposition can be achieved by excitation spectra of the characteristic emissions in combination with an analysis of the changes in absorption caused by thermal treatment. Due to the observed similarities among the studied host materials we concentrate in the following only on KCl.

### 2. Excitation spectra

Figure 5 shows the excitation spectra for two different samples. In (a) we have high $[Yb^{2+}]$ and rather low $[CN^{-}]$ concentration, and in (b) vice versa. In both cases emission from all characteristic spectral regions can be observed—blue ($\sim$450 nm), orange ($\sim$550 nm), and red ($\sim$750 nm). However, the excitation spectra show significant differences. For the case of high $[Yb^{2+}]$ and low $[CN^{-}]$ in Fig. 5(a), the two bands related to the **A** and **B** absorptions in Fig. 1(c) remain for all four emissions the dominant excitation peaks. As the probe emission wavelength is changed from blue $\rightarrow$ orange $\rightarrow$ red only fairly weak additional features appear in form of some small bands at lower energies. This suggests for this sample isolated $Yb^{2+}$ defects as the dominant centers with small enough mean distance to allow efficient resonant energy transfer among them and energy trapping in rare $Yb^{2+}$:$(CN^{-})_n$ defect complexes. These processes are drastically suppressed for lower $[Yb^{2+}]$, so that the excitation spectra should better represent the absorption of centers with different $n$ value. Indeed, the spectra for the sample with low $[Yb^{2+}]$ and high $[CN^{-}]$ in Fig. 5(b) show characteristically different shapes, and we can make intuitively the following assignment: blue $n=0$, orange $n=1$, red $n\geq2$ which we will discuss and justify below. The excitation spectra of the $CN^{-}$ vibrational luminescence (VL) in the infrared $\sim5$ $\mu$m (Fig. 5) resemble the ones for the red emission in both samples. From that we conclude, that red emission and VL originate from the same defect complex. Obviously, the $E$-$V$ energy transfer between $Yb^{2+}$ and $CN^{-}$ takes place mainly in the defect complexes with higher $n$ $(n\geq2)$.

### 3. Thermal treatments

Thermal treatments are used to partially convert one defect complex into another one providing further useful information for the decomposition of absorption spectra. As one type of sample we used the crystals which were slowly annealed from the crystal melting point to RT just after crystal growth and subsequently stored for some time ($\sim$weeks) at RT. The measured low temperature absorption spectra of these samples (Fig. 6) are compared to the one obtained just after fast quenching from $\sim150$ °C. For the KCl sample with $4\times10^{-5}Yb^{2+}$ and $5\times10^{-3}CN^{-}$ we easily see that the absorption of isolated $Yb^{2+}$ increases, while the absorption of more complex defects decreases. However, the total integrated absorption intensity does not change after thermal quenching. From these experiments, we can obtain the following important information.

(a) The defect complexes of $Yb^{2+}$:$(CN^{-})_n$ can be converted partially into simpler forms by a thermal energy of $\sim150$ °C. Obviously, the binding energy between $Yb^{2+}$ and $CN^{-}$ in KCl hosts is rather weak and similar as for pairs of rare earth defects in alkali halides.[17]

(b) The integrated oscillator strengths of $Yb^{2+}$ ions are similar, as assumed already above, for the isolated form and for the $Yb^{2+}$:$(CN^{-})_n$ defect complexes.

(c) Already at RT a slow center aggregation takes place forming preferentially $(CN^{-})_n$ related $Yb^{2+}$ complexes.

These properties are very similar to F center systems raising the hope that in analogy to these a controlled photoinduced aggregation of $Yb^{2+}$:$(CN^{-})_n$ complexes should be possible. Unfortunately, all attempts in this direction have been unsuccessful so far.

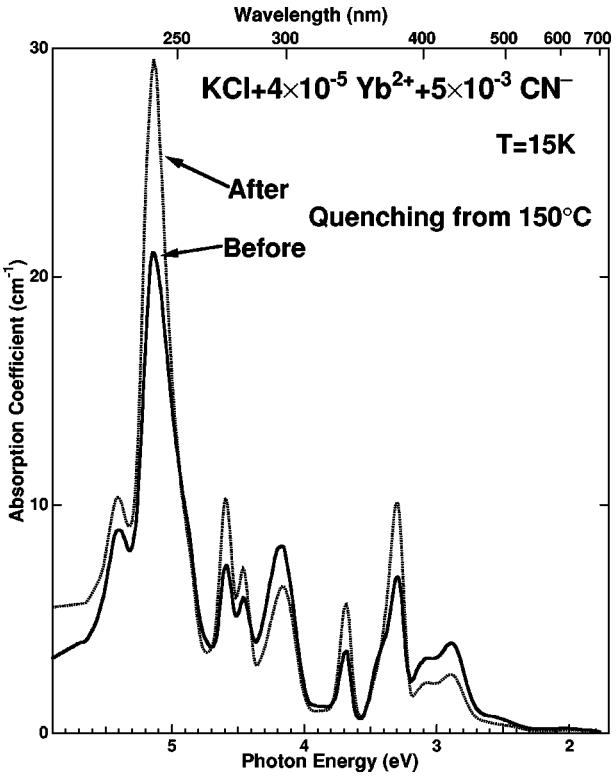


FIG. 6. Absorption spectral change of $KCl+4\times10^{-5}Yb^{2+}+5\times10^{-3}CN^{-}$ at $T=15$ K before (solid line) and after (broken line) thermal quenching from 150 °C. The absorption bands of isolated $Yb^{2+}$ defects increase after quenching.

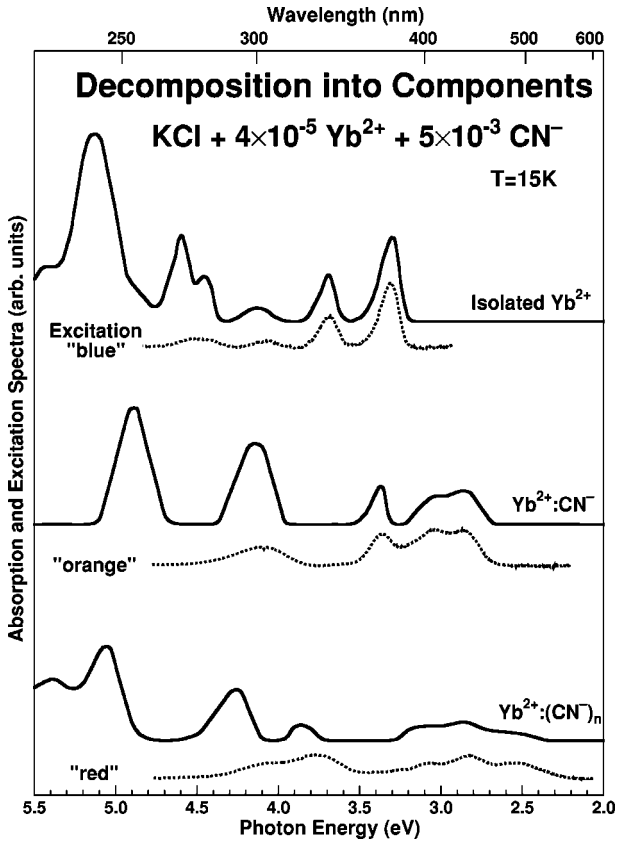


FIG. 7. Absorption spectrum of $KCl+4\times10^{-5}Yb^{2+}+5\times10^{-3}CN^{-}$ at $T=15$ K is decomposed into three components of isolated $Yb^{2+}$, $Yb^{2+}$:$CN^{-}$, and $Yb^{2+}$:$(CN^{-})_n$ with n $\geqslant 2$. These decomposed components are compared to the excitation spectra of Fig. 5(b).

#### *4. Decomposition of absorption spectra into $Yb^{2+}$:$(CN^{-})_n$*

Using the excitation spectra and the thermal treatments, we decompose the absorption spectra into different $Yb^{2+}$:$(CN^{-})_n$ defect complexes. This enabled us to separate the absorption contribution from three groups with $n=0,1$, and $n\geqslant 2$, showing the results in Fig. 7. The obtained spectra are in good agreement with the blue, orange, and red excitation spectra, respectively from Fig. 5(b). The resulting absorption spectrum for the simple $Yb^{2+}$:$CN^{-}$ defect complex (middle one of Fig. 7) consists of several bands and strongly resembles the spectrum for isolated $Yb^{2+}$ defects (bands **A**–**F**) just shifted to lower energies by 0.35–0.5 eV. Similarly, it can be seen that the whole absorption spectrum shifts further as the $n$ value increases, although a distinction between the absorption contributions of the complexes with $n=2$ and ($n\geqslant 3$) is very difficult. A crude estimate we can obtain by comparing the decomposed absorption spectra for samples with high and low $[CN^{-}]$ concentration. We find that the transition energy of $Yb^{2+}$:$(CN^{-})_2$ shifts by $\sim$0.35 eV compared to that of $Yb^{2+}$:$CN^{-}$, while the absorption bands of the more complicated complexes ($n\geqslant 3$) shift even further to lower energies. As the end-point of $n$ variation we take the defect complex of $Yb^{2+}$:$(CN^{-})_6$ measured directly without decomposition for pure KCN. The lowest energy band of its electronic absorption is located at $\sim$2.2 eV (see Fig. 3), which is about 1.1 eV lower than the **A** absorption band of isolated $Yb^{2+}$ ions ($n=0$). Therefore, the average shift of the lowest energy level for the allowed transitions is about 0.2 eV($\sim$1600 $cm^{-1}$) when the $n$ value increases by 1. However, since the energy shifts for $n=0\rightarrow1$, $1\rightarrow2$, and $2\rightarrow3$ are larger than the average, we expect that the energy shifts for $n=3\rightarrow4$, $4\rightarrow5$, and $5\rightarrow6$ are smaller than the average value. For that reason, the absorption bands of $Yb^{2+}$:$(CN^{-})_n$ defect complexes with $n=4,5$, and 6 found in samples with high $[CN^{-}]$ are expected to spectrally overlap with each other more and more making a decomposition of the absorption spectra in such samples impossible. Similar conclusion about the spectral shifts can be drawn from the emission spectra obtained in highly $CN^{-}$-doped samples which exhibit a smooth (not stepwise) shift towards lower energies with decreasing excitation energy.

## III. DISCUSSION AND SUMMARY

In this final section we discuss the drastic shift of the $Yb^{2+}$ transition energy due to the $CN^{-}$ neighbors. Since *ab initio* quantum-chemical calculations of the electronic energy levels are very complicated and beyond the scope of this paper, we apply here the more phenomenological approach of the ligand field theory which was developed in details for transition metal-ion complexes.[18,19] This approach to treat our defect system as a single entity (''pseudomolecule'') is further motivated by our observation that similar spectral absorption shifts of $Yb^{2+}$:$CN^{-}$ complexes are observed in

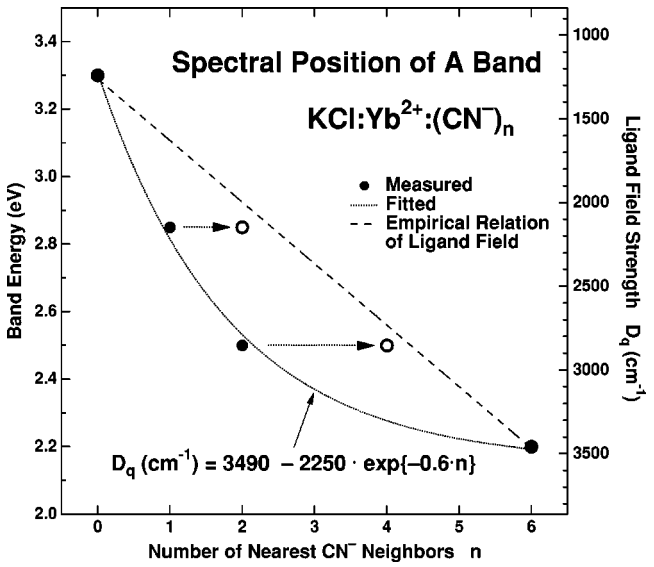


FIG. 8. Decrease of the **A** band absorption energy $Yb^{2+}$ versus the number of nearest-neighbor $CN^-$ ions in KCl. Their relation is fitted well to an exponential curve.

the melt (see Sec. II A) as well as in aqueous solution. Following the usual procedure we determine first the phenomenological ligand field strength $D_q$ for our complexes, and then try to explain their sizes with semi-quantitative arguments.

### A. Ligand field strength

As mentioned above, the ligand field theory has been applied with different kinds of modifications for the isolated $Yb^{2+}$ in alkali halides by several authors,[12,14,20] yielding an almost host-independent ligand field strength parameter $D_q$ of $\sim 1200\ cm^{-1}$. Unfortunately, a similar crystal field analysis for our $Yb^{2+}:(CN^-)_n$ is not possible because the absorption spectra could not be decomposed completely into the contribution of the different complexes over a sufficiently large spectral range. For this reason we restrict ourselves to a semiquantitative comparison based on the published energy level schemes, considering only the lowest lying transition (i.e., **A** band in absorption).

The measured energy positions of the **A** bands for our $Yb^{2+}:(CN^-)_n$ complexes are plotted on the left axis in Fig. 8 as a function of *n*. This measured **A** position can be converted into the ligand field strength parameter $D_q$ with the help of the calculated energy level diagrams (e.g., Fig. 1 of Ref. 20). Unfortunately, the published level schemes do not extent to large enough values to directly find the $D_q$ for $n=6$ in pure KCN. For approximation, the lowest energy level curve is extrapolated linearly beyond the limit of the figure ($D_q = 1800\ cm^{-1}$), and the $D_q$ values of our complexes are shown on the right axis of Fig. 8. The obtained value of $D_q \approx 3450\ cm^{-1}$ for the $Yb^{2+}:(CN^-)_6$ defect complex represents an increase of $D_q$ by a factor of $\sim 3$ under exchange of the 6 ligands from $Cl^-$ or $Br^-$ to $CN^-$.

Here we encounter again the assignment problem of the *n* values to the absorption bands of our complexes. First we test all possible integers from 0 to 6 with increasing $[CN^-]$ concentration. In this case, the experimental data (●) can then be fitted to a phenomenological relation (solid line in Fig. 8) of the following form:

$$D_q[\mathrm{cm}^{-1}] \approx 3490 - 2250 \exp(-0.6n). \tag{3.1}$$

Secondly we could speculate that the smallest complex is formed with $n=2$, similar to these observed for some other pairs of divalent cation-molecular defects [e.g., $Ca^{2+}/OH^-$ forming $Ca(OH)_2$].[21] Assuming beyond this, that only complexes with even numbers $n=0,2,4,6$ are allowed, we obtain in Fig. 8 with assignments (○) an almost linear behavior of the form

$$D_q(n) \approx \frac{n}{6} D_q(6) + \left(6 - \frac{n}{6}\right) D_q(0) \tag{3.2}$$

which is indeed expected for mixed ligands with purely electrostatic and hence additive interaction.[18] Although the second assignment appears attractive at first sight, it is ruled out by the measurements of the vibrational absorption of the complexes.[22] Moreover, the ligand-ligand interaction and covalent bonding effects play a strong role for a large difference between $D_q(0)$ and $D_q(6)$. These effects yield a behavior expressed in Eq. (3.1) with the decreasing role for every extra ligand. Beyond this it is evident that for statistical distribution of $x \leqslant 2 \times 10^{-3} CN^-$ ions formation of $n=2$ complexes with $Yb^{2+}$ ions is an order of magnitude lower than for $n=1$ pairs; thermodynamically, the $n=2$ complex could ''win the game'' only by a very strong binding energy, for which there is no evidence. In summary of these reasons, we adapt (as done already in the previous section) the first assignment.

### B. Interpretation of the large $D_q$ values

The spectral shifts and resulting $D_q$ values for our $Yb^{2+}:(CN^-)_n$ complexes are very large compared to the ones observed for other ligands present in different host materials (e.g., alkali halides,[12,13,17] alkali earth halides,[14,23,24] and alkali earth sulphates[25]). It reveals the special role of the $CN^-$ molecule as a partner of metal complexes. The only observation somewhat resembling our results is a strongly redshifted emission related to photoionization which has been found[23,26] in several host, not including the alkali halides. In those cases no shift of absorption is observed.

This strong defect partner dependence seems very unusual from the viewpoint of the $Yb^{2+}$ defects in solid state materials, but it is well known from metal-ion complexes. For such complex-molecules involving transition metal-ions and various ligands, a ''spectrochemical'' series has been empirically established by ordering the ligands according to their contribution to the $D_q$ values. In this series, the halide ions ($Cl^-, Br^-, I^-$) are on the weak ligand field side whereas $CN^-$ ligands are at the other end always causing large $D_q$. For instance, in $(CrCl_6)^{3-}$ and $[Cr(CN)_6]^{3-}$ complexes the $D_q$ values of 1360 and 2630 $cm^{-1}$ show $\sim 2$ times change which is comparable to our $Yb^{2+}:(Cl^-)_6$ and $Yb^{2+}:(CN^-)_6$ complexes.[18] The data leading to the series are taken mainly from $d \rightarrow d$ transitions of transition metal-ion complexes. However, the series also can be applied for

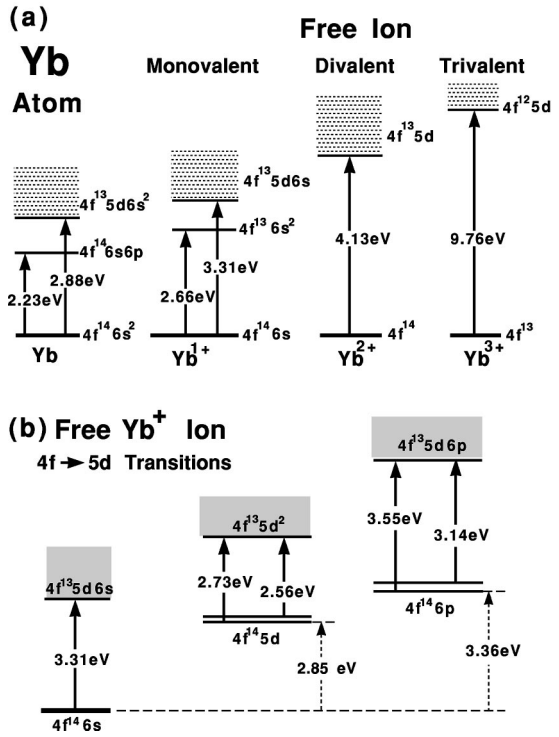


FIG. 9. Energy level diagram of $4f^{14} \rightarrow 4f^{13}5d$ electronic transitions for (a) free $Yb^{m+}$ ions under electronic valence variation (from neutral atom to trivalent ion) and (b) free $Yb^{+}$ ions under initial energy state variation.

semiquantitative arguments to the $4f \rightarrow 5d$ transitions of $Yb^{2+}$ due to the very small change of $4f$ states (i.e., $4f$ orbitals are shielded by the filled outer shells of $5s$ and $5p$). Under these conditions, an increase in the splitting of the $5d$ levels will cause a redshift of the lowest excited states. This phenomenological ''rules'' of the spectrochemical series is completely consistent with our observation. For a deeper understanding of the wide variation of ligand field strengths, both purely electrostatic and different chemical bonding effects must be taken into account.[18]

In order to get a feeling about the role of the different contributions in our system we estimate as a first step the spectral shifts by the electrostatic interaction. Using equations from Ref. 27 we find that they can only be produced by unreasonably large off-center shifts of the $CN^{-}$ ion away from the regular lattice site; therefore the electrostatic contribution can be ruled out as the sole source for the increased $D_q$ values. Obviously, our complexes exhibit strong metal-ligand exchange,[28] covalency and/or charge transfer[29] effects.

As a second step we consider a charge transfer or redistribution from the $CN^{-}$ molecules to $Yb^{2+}$ thereby adding some covalent contribution to the otherwise strongly ionic bond between the defect partners. Since firstly the electron affinity of $Yb^{2+}$ is much larger compared to the ionization energies of $CN^{-}$ and $Cl^{-}$ and secondly the $Yb^{2+}$ represents an effective positive charge within the alkali halide lattice, we expect that the redistribution of electronic charge density is directed towards the $Yb^{2+}$ ion leading to a decrease of its effective ionization. To estimate the influence of this effect we consider in Fig. 9(a) the decrease of $Yb^{2+}$ ionization in the series of free ions and atoms ($Yb^{2+} \rightarrow Yb^{+} \rightarrow Yb^{0}$) and find that indeed the $4f \rightarrow 5d$ transition energy becomes consequently reduced.

In the chemistry of metal ion complexes the covalent contribution to a bond is often discussed in terms of the ''nephelauxetic'' series which describes the electron cloud expansion of a central metal-ion due to neighboring ligands.[19] In this series (which should also hold for $5d$ levels of rare earth ions) the halide anions ($Cl^{-}$ and $Br^{-}$), are located very close to the $CN^{-}$ ion. This seems to rule out our attempt to explain the strong differences in $D_q$ for $CN^{-}$ and $Cl^{-}$ ligands by covalency. However, it was found by Mössbauer spectral measurements that while for $Eu(CN)_2$, compared to that of $EuCl_2$, the bonding character is only slightly more covalent the $5d$ orbitals of $Eu^{2+}$ are much more participating in the bonding.[30] Such data are not available for $Yb^{2+}$ but it is reasonable to assume a similar behavior due to their electronic similarity. This result encouraged us to consider the influence of the $Yb^{2+}$ orbital involved in the bond. For that purpose we show in Fig. 9(b) how the energy of the $4f \rightarrow 5d$ transitions is changed when the extra electron of a free $Yb^{1+}$ ion (added to $Yb^{2+}$) is in different orbitals. In comparison to its occupation of $6s$ or $6p$ orbitals, this transition-energy becomes strongly reduced (by 0.75 or 0.58 eV, respectively) if the electron is in a $5d$ state. This yields strong support for an interpretation that our observed large $D_q$ values are due to a redistribution of charge from the $CN^{-}$ ligands to the $5d$ orbital of the $Yb^{2+}$ ion in case of $CN^{-}$ ligands, whereas for $Cl^{-}$ and $Br^{-}$ charge is transferred to the $6s$ or $6p$ orbitals. This difference in the nature of the ''bonding'' could also explain the different relative positions of $CN^{-}$ and $Cl^{-}$ in the nephelauxetic and spectrochemical series.

In summary, we have experimentally characterized in detail the observed spectral shifts of the electronic transitions of $Yb^{2+}:(CN^{-})_n$ complexes in alkali halides and discussed them following the phenomenological ligand field theory. The found large $D_q$ values are consistent with the position of $CN^{-}$ in the spectrochemical series. More specifically we interpret the differences in $D_q$ for $CN^{-}$ and $Cl^{-}$ by the type of $Yb^{2+}$ orbital ($5d$ or $6s$) which is occupied through a charge redistribution from the respective ligand.

Despite this semiquantitative explanation of the spectral shifts, the question arises why the host-material dependence of the observed spectral changes is small, although intuitively one would expect at first that the charge redistribution depends considerably on the altered lattice constants. To understand this problem, quantum-chemical treatments of our defect complexes must be done more quantitatively which take both the charge distributions of the defect partners and the influence of the lattice into account. A promising approach could be the method of embedded molecular-cluster calculations which has been successfully used for $[Fe^{3+}(CN^{-})_6]$ in NaCl hosts.[31]

In addition to this, a question arises for the microscopic configuration and the dynamical interaction between defect partners in host lattices. To understand this, we will extend this work to the vibrational absorption (VA) of $CN^{-}$—with $Yb^{2+}$ partners and the spectroscopy of its vibrational lumi-

nescence (VL), produced by *E-V* transfer from photo-excited $Yb^{2+}$ ions.[22] Also we will further explore the time dependence of the *E-V* transfer in terms of competition between EL of $Yb^{2+}$ and VL of $CN^-$—under temperature variation.

Finally we would like to point out that the possibility to shift the emission wavelength (by a proper choice of $CN^-$ doping and/or excitation wavelength) over a wide spectral range makes these defects an attractive system for application as tunable laser sources and as phosphors. This aspect becomes even more relevant with the foreseeable wide availability of blue laser diodes and LEDs with wavelengths ($\sim$450 nm) well suited for optical excitation.[32] Experiments in this direction are currently under way.

## ACKNOWLEDGMENTS

This work was supported by NSF Grant Nos. DMR 92-23230 and DMR 96-32959. One of the authors (C.P.A.) thanks Professor H. Nakagawa for useful discussions. V.D. thanks Professors W. von der Osten and A.A. Kaplyanskii and Dr. Th. Tröster and Dr. A. Shluger for numerous discussions on the topic, and acknowledges the financial support by the University of Paderborn.

*Permanent address: Fachbereich Physik Universität Paderborn, D-33095 Paderborn, Germany.

[1] Y. Yang and F. Luty, Phys. Rev. Lett. **51**, 419 (1983).
[2] Y. Yang and F. Luty, J. Phys. (Paris) Colloq. **10**, C7 (1985).
[3] K.T. Tsen, G. Halama, and F. Luty, Phys. Rev. B **36**, 9247 (1987).
[4] V. Dierolf and F. Luty, Rev. Solid State Sci. **4**, 479 (1990).
[5] D. Samiec, H. Stolz, and W. von der Osten, Phys. Rev. B **53**, 8811 (1996).
[6] W. Gellermann, Y. Yang, and F. Luty, Opt. Commun. **57**, 196 (1986).
[7] F. Luty and V. Dierolf, in *Defects in Insulating Materials (Proceedings of ICDIM92)*, edited by O. Kanert and J.-M. Spaeth (World Scientific, Singapore, 1993), p. 17.
[8] A. Naber and F. Fischer, Radiat. Eff. Defects Solids **119-121**, 553 (1993).
[9] A. Naber, Ph.D. thesis, Westfälische Wilhelms-Universität Münster, 1993.
[10] M. Müller, J.L. Fabris, A.C. Hernandes, and M. Siu-Li, J. Lumin. **59**, 289 (1994).
[11] W. Bryant, J. Opt. Soc. Am. **55**, 771 (1965).
[12] S.W. Bland and M.J.A. Smith, J. Phys. C **18**, 1525 (1985).
[13] T. Tsubui, H. Witzke, and D.S. McClure, J. Lumin. **24&25**, 305 (1981).
[14] T.S. Piper, J.P. Brown, and D.S. McClure, J. Chem. Phys. **46**, 1353 (1967).
[15] M. Wagner and W.E. Bron, Phys. Rev. **139**, 223 (1965).
[16] T. Tsubui, D.S. McClure, and W.C. Wong, Phys. Rev. B **48**, 62 (1993).
[17] J.O. Rubio, J. Phys. Chem. Solids **52**, 101 (1991).
[18] H. Schläfer and G. Gliemann, *Basic Principles of Ligand Field Theory*, translated from the German by D. Ilten (Wiley-Interscience, London, 1969).
[19] C. Jorgensen, *Modern Aspects of Ligand Field Theory* (North-Holland, Amsterdam, 1971).
[20] M.V. Eremin, Opt. Spectrosc. **29**, 53 (1970).
[21] B. Fritz, F. Luty, and J. Anger, Z. Phys. **174**, 240 (1963).
[22] C. P. An, V. Dierolf, and F. Luty (unpublished).
[23] B. Moine, C. Pedrini, D.S. McClure, and H. Bill, J. Lumin. **40&41**, 299 (1988).
[24] S. Lizzo, A. Meijerink, G.J. Dirksen, and G. Blasse, J. Lumin. **63**, 223 (1995).
[25] S. Lizzo, A. Meijerink, and G. Blasse, J. Lumin. **59**, 185 (1994).
[26] D.S. McClure and C. Pedrini, Phys. Rev. B **32**, 8465 (1985).
[27] E. König and S. Kremer, *Ligand Field Energy Diagrams* (Plenum Press, New York, 1977).
[28] E.K. Ivoilova and A.M. Leushin, Sov. Phys. Solid State **22**, 601 (1980).
[29] B.Z. Malkin, in *Spectroscopy of Solids Containing Rare Earth Ions*, edited by A.A. Kaplyanskii and R.M. Macfarlane (Elsevier Science Publisher, Amsterdam, 1987), No. 21.
[30] I. Colquhoun, N. Greenwood, I.J. McColm, and G.E. Turner, J. Chem. Soc. Dalton Trans. **13**, 1337 (1972).
[31] P. Souchko, A. Shluger, R. Baetzold, and C.R.A. Catlow (unpublished).
[32] S. Nakamura and G. Fasol, *The Blue Laser Diode: GaN Based Emitters and Lasers* (Springer, Berlin, 1997).